Proc Indian Natn Sci Acad **79** No. 4 December 2013 Spl. Issue, Part A, pp. 563-574
© *Printed in India.*
DOI: 10.16943/ptinsa/2013/v79i4/47993

Research Paper

Elasto-Plastic Behaviour of Thick Plates with a Higher-Order Shear Deformation Theory

T KANT[1*], R K TRIPATHI[2] and V RODE[3]
[1]*Department of Civil Engineering, Indian Institute of Technology Bombay, Mumbai 400 076, India*
[2]*Department of Civil Engineering, National Institute of Technology, Raipur 492 010, India*
[3]*Department of Civil Engineering, Shri G S Institute of Technology and Science, Indore 452 003, India*

(Received 18 February 2013; Revised 21 May 2013; Accepted 25 May 2013)

A *Higher Order Shear Deformation Theory* (HOST) is utilized for elasto-plastic analysis of plate bending using *incremental finite element* formulation. Modified Newton-Raphson method has been used to solve the non-linear equations. Yielding of the material has been modelled using von Mises yield criterion, associated flow rule and isotropic hardening. Results are compared with available benchmark and other solutions. Comparisons clearly demonstrate better performance of the theory for inelastic response.

Key Words: Plate-Bending; Higher Order Theory; Elasto-Plastic Response; Incremental Finite Element Method

Introduction

Bending behaviour of plates is usually described by three mathematical models: Poisson-Kirchhoff plate theory [1], Reissner-Mindlin first order plate theories [2-4] and higher order plate theories [5-9]. Poisson-Kirchhoff theory, which is also known as *Classical Plate Theory* (CPT), is based on assumption that straight lines perpendicular to mid-surface (i.e., transverse normals) before deformation remain straight and normal to the mid-surface and undergo no change in length during deformation. These assumptions imply that the transverse normal strain ε_z and transverse shear strains and are zero. It can also be easily shown that CPT is computationally inefficient (requires C^1 continuity of transverse displacement) from the simple finite element formulation's point of view.

The first order shear deformation theories (FOSTs), which include transverse shear deformation, can be classified on the basis of the assumed field as (i) stress-based theories and (ii) displacement-based theories. Reissner [2, 4] and Mindlin [3] are the two pioneers to provide first order shear deformation theories based on the assumed stress and assumed displacement variations through the thickness of the plate, respectively. These theories provide a first-order basis for the consideration of the transverse shear deformation effect and required a C^o continuous finite element formulation for the numerical analysis. However, FOSTs have following limitation:

- The transverse shearing strains/stresses turn out to be constant through the plate thickness and a fictitious shear correction coefficient is introduced to correct the shear energy.

Lo *et al.* [5] have presented a theory for plates based on assumed higher-order displacement field. Kant [6] has derived an isotropic version of the complete governing equations of such a theory based

*Author for Correspondence: E-mails: tkant@civil.iitb.ac.in, rajesh_tripathi64@yahoo.co.in, vrode@sgsits.ac.in

on the minimum potential energy principle. A C^0 finite element formulation of this higher order theory is presented, for the first time, by Kant *et al.* [7]. In this theory, the in-plane displacements are expanded in the powers of the thickness coordinate (z) by Taylor series, which allows:

- Quadratic variation of the transverse shearing strains through the plate thickness avoiding the introduction of a shear correction coefficient.
- Warping of the cross-section is automatically incorporated.

When the plate is loaded beyond elastic limit, the plastic strain occurs, which causes a redistribution of stresses. The computation of this redistribution was not an easy task before digital computers arrived. Hence modelling of plastic behaviour started as limit analysis and then switched over to incremental non-linear analysis. Initially for a long span of time, limit analysis was used for the plastic analysis of beams and frames due to their linear idealisation. Simplicity of their formulation leads to the collapse loads. Plates, due to their two-dimensional idealisation, make the problem complicated and in most of the cases lead to the upper and lower bounds to the collapse loads instead of collapse loads themselves. The axisymmetrically loaded, circular plates were the simplest problem to begin with, and therefore attracted the attention of many researchers. Sokolovsky [10] was considered to be the pioneer amongst them. He dealt with the non-linear bending of simply supported circular plates with small displacements and thin plate assumptions. He used the Hencky's deformation theory for a strain-hardening material obeying von Mises yield criterion. Pell and Prager [11], Hopkins and Prager [12] and Hopkins and Wang [13] predicted the load-carrying capacities of circular plates of a perfectly plastic material and subjected to rotationally symmetric loads for various support conditions. The initial works were confined to the circular plate case. Hodge [14] took the research out of this barrier by presenting the procedure of finding the bounds of non-circular plates. The previous researches mostly used Tresca yield criterion since the directions of principal moments were already known for circular plates due to radial symmetry. This was not the case with the rectangular plates and therefore the von Mises yield criterion was used for thin plates of perfectly plastic material and presented the bounds for a simply supported square plate under uniform load as a special case. Hodge and Belytschko [15] formulated upper and lower bound problem as a mathematical programming problem, but by using finite element representations of velocity and moment fields insuring the satisfaction of yield condition throughout the plate. The plastic limit loads of the clamped circular plate have been presented by Guowel *et al.* [16] based on unified yield criterion.

The limit analysis is applicable to rigid perfectly plastic behaviour while almost all the materials are elastic before yielding. The current state of stress in a yielded material again depends upon the history of loading. Therefore, an analysis starting from the loading in the elastic range and gradually increasing to plastic range till failure would be closer to the true behaviour of the plate.

Haythornthwaite [17] was the first to use an incremental method for the elasto-plastic analysis of plates. He computed the deflections of plates with circular symmetry for an elastic-plastic material. Comparison was made with predicted limit loads of Hopkins and Prager [12]. Armen *et al.* [18] developed a finite element technique for plastic bending by additionally considering in-plane stresses and geometric nonlinearity. They developed the formulation by interpreting plastic strains as initial strains and using stress-strain relations from incremental plasticity theory. Material behaviour was based on von Mises yield criterion with Prager-Zieglar kinematic hardening. Dinis *et al*. [19] considered the semiloof shell element for elasto-plastic large displacement analysis of plates and shells. An initial stiffness plasticity algorithm and elasto-plastic model was considered for the material non-linear analysis.

Owen and Figueiras [20] extended the application of semiloof element analysis to include the effect of transverse shear by deriving a shear correction coefficient for cylindrical bending with the assumption of constant transverse shear strains. Reddy and Chandrashekhara [21] derived a non-linear version of Sander's first-order shear-deformation shell theory

accounting for von Karmann's strains and Hill's anisotropic yield criterion for the elasto-plastic bending analysis of plates and shells.

Watanabe and Kondo [22] further consolidated their earlier (Kondo and Watanabe [23]) work by considering more numerical examples and better comparisons. They derived the elastic-plastic incremental tangent stiffness matrix without numerical integration over the area of the elements using the nodal displacements and nodal forces as fundamental variables instead of generalised strains and stresses respectively.

Papadopoulos and Taylor [24] developed an inelastic finite element analysis of plates, which includes the effects of transverse shear-deformation. They used the Reissner-Mindlin's plate bending theory and an elasto-plastic constitutive model in the stress-resultant form based on generalisation of Von Mises plane stress criterion and associated flow rule. The plastic constitutive rate equations were integrated by a return-mapping algorithm and solved incrementally using a Newton method. Prasad and Sridhar [25] have developed an elasto-plastic finite element procedure using degenerated shell element with assumed strain field technique, von Mises yield criteria and isotropic hardening. They have demonstrated the correctness and applicability of the method by numerical examples.

The dependency of incremental elasto-plastic analysis on loading history required the use of an accurate elastic plate bending theory.

In the present study a special HOST model which includes distortion of the transverse normal is utilized for elasto-plastic analysis of plate bending. von Mises criterion [26], associated flow rule and isotropic hardening have been used in the formulation. The modified Newton-Raphson's [27] method has been used for solution of non-linear equations.

A Higher-Order Shear Deformation Theory

The development of the present theory starts with the assumption of the displacement field in the following form [6, 7]:

$$\begin{aligned} u(x,y,z) &= z\theta_x(x,y) + z^3\theta_x^*(x,y) \\ v(x,y,z) &= z\theta_y(x,y) + z^3\theta_y^*(x,y) \\ w(x,y,z) &= w_0\,(x,y) \end{aligned} \tag{1}$$

The terms have usual meaning except the terms θ_x^* and θ_y^* which are the corresponding higher order terms in the Taylor's series expansion. The transverse displacement component 'w' has only one term 'w_0' and thus disregards transverse normal deformation.

Strain-Displacement Relationships

The linear relationships between these displacements and strains can be obtained by using the definitions of strains from the theory of elasticity:

$$\left.\begin{aligned} \varepsilon_x &= \frac{\partial u}{\partial x} = z\chi_x + z^3\chi_x^* \\ \varepsilon_y &= \frac{\partial v}{\partial y} = z\chi_y + z^3\chi_y^* \\ \varepsilon_z &= 0 \\ \gamma_{xy} &= \frac{\partial u}{\partial y} + \frac{\partial v}{\partial x} = z\chi_{xy} + z^3\chi_{xy}^* \\ \gamma_{yz} &= \frac{\partial v}{\partial z} + \frac{\partial w}{\partial y} = \phi_y + z^2\phi_y^* \\ \gamma_{zx} &= \frac{\partial u}{\partial z} + \frac{\partial w}{\partial x} = \phi_x + z^2\phi_x^2 \end{aligned}\right\} \tag{2}$$

where,

$$\left.\begin{aligned} \left(\chi_x, \chi_y, \chi_{xy}\right) &= \left(\frac{\partial\theta_x}{\partial x},\ \frac{\partial\theta_y}{\partial y},\ \frac{\partial\theta_x}{\partial y} + \frac{\partial\theta_y}{\partial x}\right) \\ \left(\chi_x^*, \chi_y^*, \chi_{xy}^*\right) &= \left(\frac{\partial\theta_x^*}{\partial x},\ \frac{\partial\theta_y^*}{\partial y},\ \frac{\partial\theta_x^*}{\partial y} + \frac{\partial\theta_y^*}{\partial x}\right) \\ \left(\phi_x, \phi_y, \phi_x^*, \phi_y^*\right) &= \left(\theta_x + \frac{\partial w_0}{\partial x},\ \theta_y + \frac{\partial w_0}{\partial y},\ 3\theta_x^*,\ 3\theta_y^*\right) \end{aligned}\right\}$$

The flexural and transverse shear strains in the plate can be written in the concise matrix form as:

$$\varepsilon_f = \begin{Bmatrix} \varepsilon_x \\ \varepsilon_y \\ \gamma_{xy} \end{Bmatrix} = z\begin{Bmatrix} \chi_x \\ \chi_y \\ \chi_{xy} \end{Bmatrix} + z^3\begin{Bmatrix} \chi_x^* \\ \chi_y^* \\ \chi_{xy}^* \end{Bmatrix} = z\chi + z^3\chi^*$$

and $$\varepsilon_s = \begin{Bmatrix} \gamma_{yz} \\ \gamma_{xz} \end{Bmatrix} = \begin{Bmatrix} \phi_y \\ \phi_x \end{Bmatrix} + z^2\begin{Bmatrix} \phi_y^* \\ \phi_x^* \end{Bmatrix} = \phi + z^2\phi^* \tag{3}$$

Stress-Strain Relations

Assuming normal stress σ_z to be negligibly small compared to other normal stresses, the constitutive matrix takes the form:

$$\boldsymbol{C} = \frac{E}{1-\nu^2}\begin{bmatrix} 1 & & & & \\ \nu & 1 & & sym. & \\ 0 & 0 & \frac{1-\nu}{2} & & \\ 0 & 0 & 0 & \frac{1-\nu}{2} & \\ 0 & 0 & 0 & 0 & \frac{1-\nu}{2} \end{bmatrix} \quad (4)$$

The stress-strain relationship in the matrix form,

$$\begin{Bmatrix}\sigma_x\\ \sigma_y\\ \tau_{xy}\end{Bmatrix} = \begin{bmatrix} Q_{11} & & sym. \\ Q_{21} & Q_{22} & \\ Q_{31} & Q_{32} & Q_{33}\end{bmatrix} z \begin{Bmatrix}\chi_x\\ \chi_y\\ \chi_{xy}\end{Bmatrix} + \begin{bmatrix} Q_{11} & & sym. \\ Q_{21} & Q_{22} & \\ Q_{31} & Q_{32} & Q_{33}\end{bmatrix} z^3 \begin{Bmatrix}\chi_x^*\\ \chi_y^*\\ \chi_{xy}^*\end{Bmatrix} \quad (5a)$$

and

$$\begin{Bmatrix}\tau_{yz}\\ \tau_{zx}\end{Bmatrix} = \begin{bmatrix} Q_{44} & Q_{45} \\ Q_{45} & Q_{55}\end{bmatrix} \begin{Bmatrix}\phi_y\\ \phi_x\end{Bmatrix} + \begin{bmatrix} Q_{44} & Q_{45} \\ Q_{45} & Q_{55}\end{bmatrix} z^2 \begin{Bmatrix}\phi_y^*\\ \phi_x^*\end{Bmatrix} \quad (5b)$$

where,

$$Q_{11} = \frac{E}{1-\nu^2} = Q_{22}, Q_{21} = \frac{\nu E}{1-\nu^2}, Q_{31} = Q_{32} = 0,$$
$$Q_{33} = G = Q_{44} = Q_{55} \text{ and } Q_{45} = 0$$

Energy Expression and Plate Constitutive Relations

The total potential energy of the plate with volume V and surface area A can be written as:

$$\Pi = U - W = \frac{1}{2}\int_V \varepsilon^T \sigma \, dV - \int_A \delta^T \mathbf{P} dA \quad (6)$$

Here *U* is the strain energy of the plate, *W* is the work done by the external forces and **P** is the vector of force intensities corresponding to generalised displacement vector ⇕ defined at the mid-surface. Substituting the expressions for strain components in the above equation and integrating through the plate thickness '*h*', one gets:

$$\Pi = \frac{1}{2}\int_A \hat{\varepsilon}^T \hat{\sigma} \, dA - \int_A \delta^T \mathbf{P} dA \quad (7)$$

in which,

$$\left.\begin{aligned} \delta &= (w_0, \theta_x, \theta_y, \theta_x^*, \theta_y^*)^T \\ \hat{\varepsilon} &= (\chi_x, \chi_y, \chi_{xy}, \chi_x^*, \chi_y^*, \chi_{xy}^*, \phi_x, \phi_y, \phi_x^*, \phi_y^*)^T \\ \hat{\sigma} &= (M_x, M_y, M_{xy}, M_x^*, M_y^*, M_{xy}^*, Q_x, Q_y, Q_x^*, Q_y^*)^T \end{aligned}\right\} \quad (8)$$

Constitutive relations in terms of stress-resultants can be written in the matrix form as:

$$\begin{Bmatrix} M_x \\ M_y \\ M_{xy} \\ M_x^* \\ M_y^* \\ M_{xy}^* \end{Bmatrix} = \left[\begin{array}{ccc:c:ccc} Q_{11}H_3 & & & & & & \\ Q_{21}H_3 & Q_{22}H_3 & & sym. & & & \\ Q_{31}H_3 & Q_{32}H_3 & Q_{33}H_3 & & & & \\ \hdashline Q_{11}H_5 & Q_{21}H_5 & Q_{31}H_5 & Q_{11}H_7 & & & \\ Q_{21}H_5 & Q_{22}H_5 & Q_{32}H_5 & Q_{21}H_7 & Q_{22}H_7 & & \\ Q_{31}H_5 & Q_{32}H_5 & Q_{33}H_5 & Q_{31}H_7 & Q_{32}H_7 & Q_{33}H_7 & \end{array}\right] \begin{Bmatrix} \chi_x \\ \chi_y \\ \chi_{xy} \\ \chi_x^* \\ \chi_y^* \\ \chi_{xy}^* \end{Bmatrix} \quad (9a)$$

and,

$$\begin{Bmatrix} Q_x \\ Q_y \\ Q_x^* \\ Q_y^* \end{Bmatrix} = \left[\begin{array}{cc:c:cc} Q_{55}H_1 & & & & \\ Q_{45}H_1 & Q_{44}H_1 & sym. & & \\ \hdashline Q_{55}H_3 & Q_{45}H_3 & Q_{55}H_5 & & \\ Q_{45}H_3 & Q_{44}H_3 & Q_{45}H_5 & Q_{44}H_5 & \end{array}\right] \begin{Bmatrix} \phi_x \\ \phi_y \\ \phi_x^* \\ \phi_y^* \end{Bmatrix} \quad (9b)$$

in which, $H_i = \frac{1}{i}\left[\left(\frac{h}{2}\right)^i - \left(-\frac{h}{2}\right)^i\right], \quad i = 1, 3, 5, 7$

Writing in a more concise form, we have

$$\begin{Bmatrix} \mathbf{M} \\ \mathbf{M}^* \\ \mathbf{Q} \\ \mathbf{Q}^* \end{Bmatrix} = \left[\begin{array}{c:c} \mathbf{D}_f & 0 \\ \hdashline 0 & \mathbf{D}_s \end{array}\right] \begin{Bmatrix} \chi \\ \chi^* \\ \phi \\ \phi^* \end{Bmatrix} \quad (10)$$

or, $\hat{\boldsymbol{\sigma}} = \mathbf{D} \ \hat{\boldsymbol{\varepsilon}}$ (10a)

Elasto-Plastic Analysis

After establishing an accurate basis of the overall elasto-plastic constitutive relations for the plate in the

elastic range by including the higher-order terms for stress-resultants, curvatures etc., and the start of the plasticity is marked by the yielding of the material. An initial yield condition, a hardening rule and a flow rule specify the plastic response of a strain-hardening material. The initial yield specifies the states of stress at which plastic deformation first occurs and may be considered a multi-axial generalisation of the yield point in a simple tension test. The hardening rule describes the modification of the yield condition due to strain hardening during plastic flow. The flow rule permits the determination of plastic strain rates at each point in the progressive loading history.

Yield Criteria for Bending of Plates

Assuming the yield function $\hat{F}$ to be a function of bending moments $\hat{\sigma}_f$ but not of shear forces $\hat{\sigma}_s$ the plate bending yield criterion [27] is given by

$$\hat{F}(\hat{\sigma}_f, \hat{\kappa}) = \int_{-h/2}^{+h/2} F(\sigma_f, \kappa) z \, dz, \tag{11}$$

Neglecting the through-the-thickness stresses σ_z, τ_{xz} and τ_{yz} for the plate, the Von-Mises criterion for the initial yield is:

$$\sigma_x^2 - \sigma_x \sigma_y + \sigma_y^2 + 3\tau_{xy}^2 = \sigma_0^2$$

Replacing by (σ_x, σ_y and τ_{xy}) (M_x, M_y by M_{xy}) and σ_0 by $M_p = \dfrac{\sigma_0 h^2}{4}$ in the above equation, Von-Mises criterion in terms of stress-resultants becomes:

$$M_x^2 - M_x M_y + M_y^2 + 3M_{xy}^2 = M_p^2 \tag{12}$$

Hardening Rules

The Isotropic Hardening [28], in which the initial yield surface uniformly expands without distortion and translation, has been considered. The equation for the subsequent yield surface can thus be written as:

$$\hat{f}(\hat{\sigma}_{ij}) = \hat{\kappa}^2(\hat{\varepsilon}_p) \tag{13}$$

in which $\hat{\kappa}^2$, whose value depends upon plastic mid-plane strain history, governs the size of the yield surface.

Flow Rule

The differentiation of elastic potential function (i.e., the complimentary energy density function) with respect to stress-resultants $\hat{\sigma}_{ij}$ gives the elastic mid-plane strains, a plastic potential function '$g(\hat{\sigma}_{ij}, \hat{\varepsilon}_{ij}^p, \hat{\kappa})$' may be similarly considered for the plastic mid-plane strain increments. Thus the plastic flow [27, 28] rule may be defined as:

$$d\hat{\varepsilon}_{ij}^p = d\lambda \frac{\partial g}{\partial \hat{\sigma}_{ij}} \tag{14}$$

in which $d\lambda$ is a positive scalar function, which is nonzero only when plastic deformations, occur and which varies throughout the history of plastic mid-plane straining. The loading parameter $d\lambda$ gives the length or the magnitude of the plastic mid-plane strain increment vector $d\hat{\varepsilon}_{ij}^p$, while the gradient of the plastic potential surface $\dfrac{\partial g}{\partial \hat{\sigma}_{ij}}$ gives the direction.

Looking at the similarity of the properties of plastic potential and yield function, they may be assumed to be actually identical.

$$g(\hat{\sigma}_{ij}, \hat{\varepsilon}_{ij}^p, \hat{\kappa}) = \hat{F}(\hat{\sigma}_{ij}, \hat{\varepsilon}_{ij}^p, \hat{\kappa})$$

and therefore,

$$d\hat{\varepsilon}_{ij}^p = d\lambda \frac{\partial \hat{F}}{\partial \hat{\sigma}_{ij}} \tag{15}$$

i.e., the plastic flow develops along the normal $\dfrac{\partial \hat{F}}{\partial \hat{\sigma}_{ij}}$ to the current yield surface (called the normality condition). The above relation (15) associates the plastic flow with the current yield surface hence it is called the 'associated flow rule' and it has been used in the present formulation.

Elasto-Plastic Incremental Stress-Resultants/ Mid-Plane Strains Relationship

The material behaves partly elastic and partly plastic after the initial yield. In case of plate bending, as discussed earlier, the stresses can be replaced by stress-resultants and strains can be replaced by the mid-plane strains. The change of mid-plane-strain during any increment in the stress-resultant can be divided into elastic and plastic components such that:

$$d\hat{\varepsilon}_{ij} = d\hat{\varepsilon}^{e}_{ij} + d\hat{\varepsilon}^{p}_{ij} \tag{16}$$

The elastic mid-plane strain increments and the stress-resultant increments are related as:

$$\begin{Bmatrix} \mathrm{d}\hat{\boldsymbol{\sigma}}_{\mathbf{f}} \\ \mathrm{d}\hat{\boldsymbol{\sigma}}_{\mathbf{s}} \end{Bmatrix} = \begin{bmatrix} \hat{\mathbf{D}}_{\mathbf{f}} & 0 \\ 0 & \hat{\mathbf{D}}_{\mathbf{s}} \end{bmatrix} \begin{Bmatrix} \mathrm{d}\hat{\boldsymbol{\varepsilon}}_{\mathbf{f}} \\ \mathrm{d}\hat{\boldsymbol{\varepsilon}}_{\mathbf{s}} \end{Bmatrix} \tag{17}$$

or, $$\mathrm{d}\hat{\boldsymbol{\varepsilon}}_{\mathbf{ij}} = \mathbf{D}^{-1}\, \mathrm{d}\hat{\boldsymbol{\sigma}}_{\mathbf{ij}} \tag{18}$$

The plastic stress-strain relations are given by the flow rule in the form of a relation between plastic mid-plane strain increment and the current yield function in case of plate bending as given in equation (15).

Thus, the complete incremental relationship between the stress-resultants and the corresponding mid-plane-strains for the elasto-plastic deformation is:

$$\mathrm{d}\hat{\boldsymbol{\varepsilon}} = \mathbf{D}^{-1}\, \mathrm{d}\hat{\boldsymbol{\sigma}} + d\lambda \frac{\partial \hat{\mathbf{F}}}{\partial \hat{\boldsymbol{\sigma}}} \tag{19}$$

After proper substitution one gets the complete elasto-plastic flexural stress-resultant curvature relationship as:

$$\mathrm{d}\boldsymbol{\sigma}_{\mathbf{f}} = \hat{\mathbf{D}}^{\mathbf{ep}}_{\mathbf{f}} \mathrm{d}\hat{\boldsymbol{\varepsilon}}_{\mathbf{f}} \tag{20}$$

and

$$\hat{\mathbf{D}}^{\mathbf{ep}}_{\mathbf{f}} = \hat{\mathbf{D}}_{\mathbf{f}} - \frac{\hat{\mathbf{D}}_{\mathbf{f}}\ \hat{\mathbf{a}}\ \hat{\mathbf{a}}^{\mathbf{T}}\ \hat{\mathbf{D}}_{\mathbf{f}}}{H + \hat{\mathbf{a}}^{\mathbf{T}}\ \hat{\mathbf{D}}_{\mathbf{f}}\ \hat{\mathbf{a}}}$$

where,

$$\hat{\mathbf{a}} = \left[\frac{\partial \hat{F}}{\partial M_x}, \frac{\partial \hat{F}}{\partial M_y}, \frac{\partial \hat{F}}{\partial M_{xy}} \right]^{\mathrm{T}},$$

$$\hat{\mathbf{D}}_{\mathbf{f}} = \int_{-h/2}^{+h/2} \mathbf{D}_{\mathbf{f}}\ \ z\ \ dz \text{ and } \hat{\mathbf{D}}_{s} = \int_{-h/2}^{+h/2} \mathbf{D}_{s}\ \ dz$$

Solution of Nonlinear Equilibrium Equation

The incremental equilibrium equation [27, 28] for the plate can be written at some stage in the solution (i.e., at any iteration during a load increment) as

$$\psi(d^p) + \boldsymbol{K_T}(d^p)\, \Delta\, d^p = 0 \tag{21}$$

where, $\psi(d^p)$ is residual force and $\boldsymbol{K_T}(d^p)$ is the tangential stiffness matrix.

$$\mathbf{K}_{\mathbf{T}} = \int_{\mathbf{A}} [\ [\mathbf{B}_{\mathbf{f}}]^{\mathbf{T}} [\hat{\mathbf{D}}^{\mathrm{ep}}]_{\mathbf{f}}\, \mathbf{B}_{\mathbf{f}} + [\mathbf{B}_{\mathbf{s}}]^{\mathbf{T}}\, \hat{\mathbf{D}}_{\mathbf{s}} \mathbf{B}_{\mathbf{s}}]\mathrm{dA} \tag{22}$$

Finite Element Formulation

In the present finite element formulation [28-30] 9-node heterosis [31] element is used. The heterosis element is formulated using 9-node Lagrangian shape functions for rotations, and 8-node Serendipity shape functions for lateral displacements. The heterosis element has the improved characteristics and gives a better consistency in performance as compared to the parent elements in a wide range of problems. In case of very thin plates with selective integration [32, 33] *shear locking* is avoided.

The Incremental Finite Element Solution Procedure

The incremental iterative finite element solution [28] with modified Newton-Raphson procedure has been adopted. While yielding, the normality condition for the increments in stress-resultants has been preserved. The convergence norms have been applied for both residual forces and displacements.

Numerical Results

A convergence study is first conducted on square and circular plates to decide the appropriate plate discretisation for further elasto-plastic study. The

convergence results are presented in Tables 1-3. For circular plates, discretisation scheme used by Liu *et al*. [34] has been used to produce least shape-distorted elements. Based on the convergence study, 16 elements and 32 elements meshes have been used for one quarter of square and circular plates respectively.

The validity and accuracy of the HOST formulation has been tested by performing the linear elastic analysis and comparing the present results with the available exact three-dimensional elasticity and other benchmark solutions for simply supported and clamped square plates. The central displacements, for comparison of plates with different thicknesses, have been normalised as:

$$\bar{w}_c = w_c \times \frac{E\ h^3}{q_0 a^4}$$

where, w_c is the actual transverse displacement at the centre of the plate, E is the modulus of elasticity of the plate material, q_0 is the uniformly distributed transverse load over the plate, a is the length of the side and h is the thickness of the plate.

Results presented in Tables 4 and 5 clearly indicate that the HOST results are very close to three-dimensional results. Hence, it is suitable for further investigation in the elasto-plastic range.

In elasto-plastic study all results have been compared with the existing analytical solutions (either exact or in the form of upper and lower bounds). The nondimensional expressions used for the normalised displacements, normalised uniformly distributed loads and normalised point loads are $\bar{w}_c = w_c D / a^2 M_p$, $\bar{q} = q_0 a^2 / M_p$ and $\bar{p} = p_0 / M_p$ respectively. Where, p_0 is the point load at centre, $D[=Eh^3/12(1-\nu^2)]$ is the flexural rigidity of the plate and M_p [$= \sigma_0 h^2/4$] is the fully plastic moment. For circular plates these expressions remain same except radius 'R' replaces

Table 1: Convergence of elastic displacements for a clamped square plate subjected to uniformly distributed load (E = 10.92, ν = 0.3, G = 4.2, h = 0.1 and a = 10.00)

Mesh	Normalised central displacement ($\bar{w}_c = w_c$ D/q_0 a^4)		
	Papadopoulos & Taylor [35]	HOST	Exact solution Liu *et al.* [34]
1 x 1	0.0018921	0.0015433	
2 x 2	0.0014834	0.0012389	
3 x 3	-	0.0012575	0.001264
4 x 4	0.0013285	0.0012641	
8 x 8	0.0012834	0.0012677	
16 x 16	0.0012718	0.0012678	

Table 2: Convergence of elastic displacements for a simply supported square plate subjected to a point load at centre (E = 10.92, ν = 0.3, G = 4.2, h = 0.1, and a = 10.00)

Mesh	Normalised central displacement ($\bar{w}_c = w_c$ D / P_0 a^2)			
	Ibrahimbegovic & Frey [36]	Wanji & Cheung [37]	HOST	Exact solution Liu *et al*. [34]
1 x 1	-	0.01127	0.01053	
2 x 2	0.01170	0.01180	0.01144	
3 x 3	-	-	0.01156	0.011603
4 x 4	0.01160	0.01169	0.01159	
8 x 8	0.01161	0.01165	0.01159	
16 x 16	0.01162	-	0.01162	

Table 3: Convergence of elastic displacements of a clamped circular plate subjected to uniformly distributed load (E = 10.92, ν = 0.3, G = 4.2, h = 1.0, and R = 5.00)

No. of elements	Normalised central displacement ($\bar{w}_c = w_c$ D/q_0 a^4)		
	Papadopoulos & Taylor [35]	HOST	Exact solution
03	0.001179	0.000946	
12	0.001169	0.001098	
20	-	0.001138	0.001155
32	-	0.001151	
48	0.001161	0.001159	
144		0.001159	

Table 4: Elastic deflection of a simply supported square plate subjected to uniformly distributed load

a/h	Exact 3D Srinivas and Rao [38]	Reddy [9]	Savithri [39]	FOST	HOST	Elastic nondimensional central displacement
05	-	0.0535	0.0536	0.0535	0.0535	$\bar{w}_c = w_c \times \frac{Eh^3}{q_0 a^4}$
10	0.0464	0.0467	0.0467	0.0467	0.0466	
20	0.0449	-	0.0449	0.0449	0.0449	
100	-	0.0444	0.0444	0.0440	0.0442	

Table 5: Elastic deflection of a clamped square plate subjected to uniformly distributed load

a/h	Exact 3D Srinivas and Rao [38]	Savithri [39]	FOST	HOST	Elastic nondimensional central displacement
05	0.02331	0.02261	0.02351	0.02352	$\bar{w}_c = w_c \times \frac{Eh^3}{q_0 a^4}$
10	0.01634	0.01602	0.01640	0.01641	
20	0.01447	0.01436	0.01449	0.01449	
100	0.01375	0.01383	0.01384	0.01373	

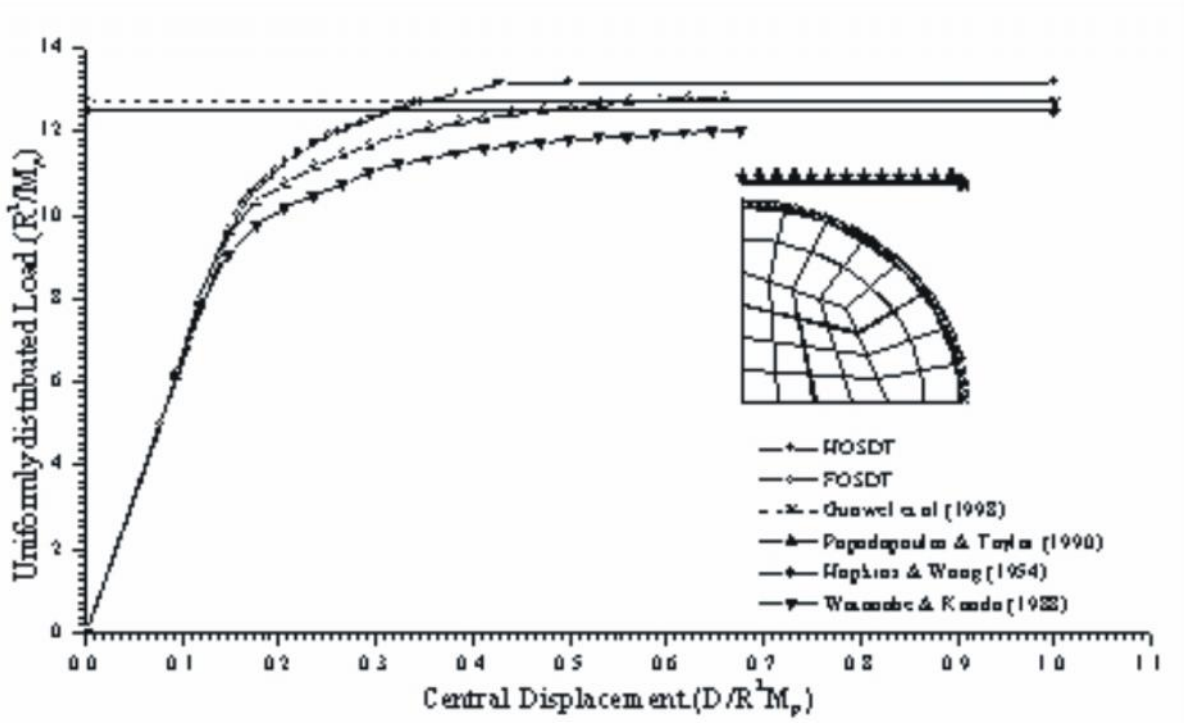

Fig. 1: Normalised load *versus* normalised central displacement for clamped circular plate with uniformly distributed load: Comparisons of different formulations for d/h=100

the side of plate 'a'. A series of problems from thick plate to thin plate are analysed to demonstrate versatility of the HOST.

FOST results are based on Reissner-Mindlin plate bending which include transverse shear deformation without warping of transverse cross

sections. A shear correction coefficient of 5/6 is used here.

Clamped Circular Plate with Uniformly Distributed Load

Fine discretization for converged solution were first established. In Table 6, normalised collapse loads have been presented for thick to thin plates and compared with the other results in the thin plate range. It is observed that, the HOST predicts normalised collapse load higher than the other finite element results as well as limit analysis results for all values of d/h. Fig. 1 shows comparison of normalised displacements versus normalised uniformly distributed loads for different formulations. In the elastic range the variation is almost similar for all formulations. Deviations are observed in the normalised load-displacement curves, by different formulations, after inception of yielding. HOST predicts highest collapse load as compared to other available results. The other formulations are based on either FOST or CPT.

Normalised load-displacement results have been represented, for different d/h ratios, in Fig. 2. It is observed that, the difference between moderately thick to thin plates (d/h = 10, 15, 20, 50, 80 and 100) is less in comparison to the difference between thick (d/h = 5) and thin (d/h = 100) plates. This difference gradually reduces in plastic region and the curves for all thicknesses appear to be converging to almost the same collapse load.

Initiation and spread of plastic zones with respect to load increments have been presented in Fig. 3 for d/h = 20. In this case, formation of plastic zone starts at the clamped edge followed by the formation of another zone at the centre with further load increments. The central plastic zone then spreads faster than the edge plastic zone. It is also observed that, a number of elements remain unyielded up to pre-collapse and then suddenly yield and lead to collapse. Thus, the final collapse takes place only after yielding of all the Gauss points.

Clamped Square Plate with Uniformly Distributed Load

Normalised collapse loads have been presented for thick to thin plates and compared with the other results in the thin plate range in Table 7. It is observed that HOST predicts normalised collapse load slightly higher than the upper bound for thin plate range.

In Fig. 4 normalised uniformly distributed loads *versus* normalised central displacements have been plotted and compared with the results given in Owen

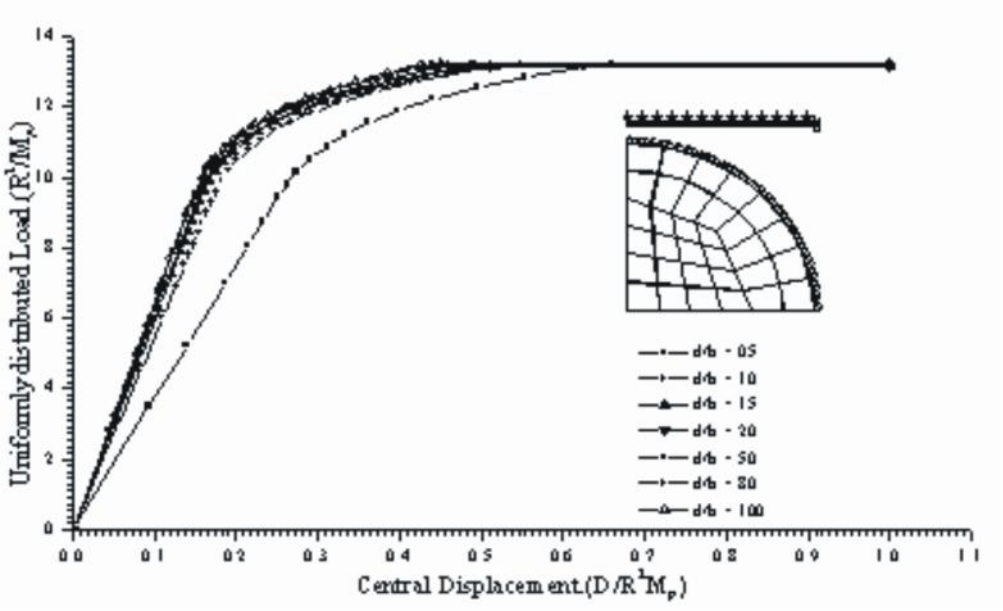

Fig. 2: Normalised load *versus* normalised central displacement for clamped circular plate with uniformly distributed load: Comparisons of different d/h ratios (HOST)

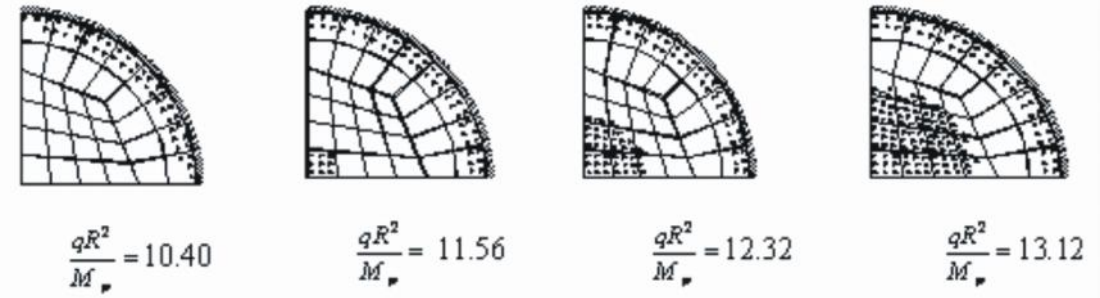

Fig. 3: Progress of plastic zone with load increments for d/h=20: Clamped circular plate with uniformly distributed load (HOST)

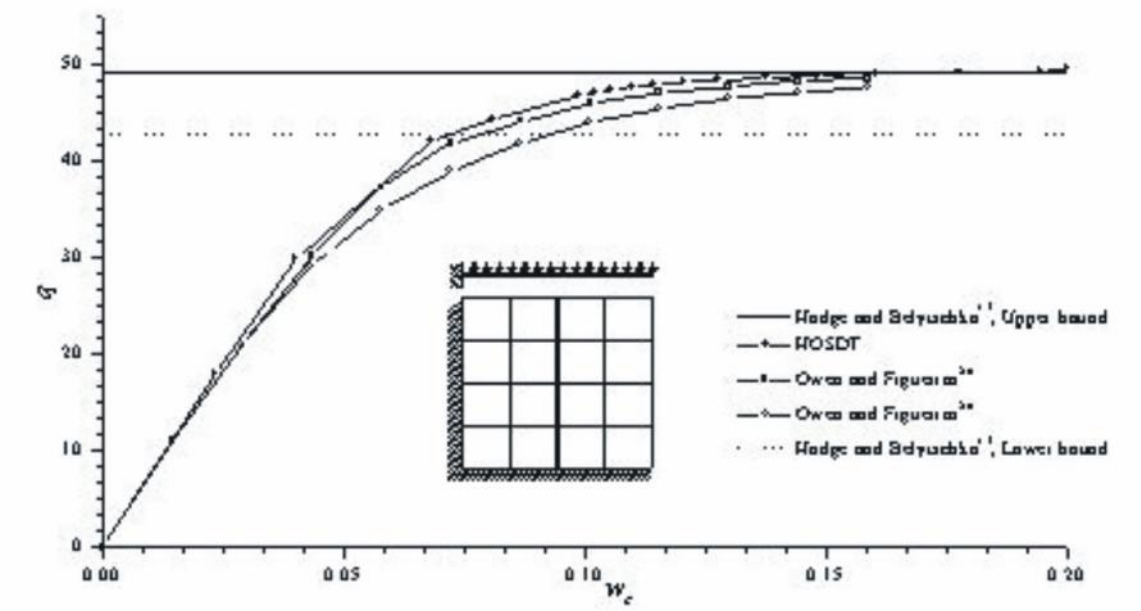

Fig. 4: Normalised load *versus* normalised central displacement for clamped circular plate with uniformly distributed load: Comparisons of different formulations for a/h=30

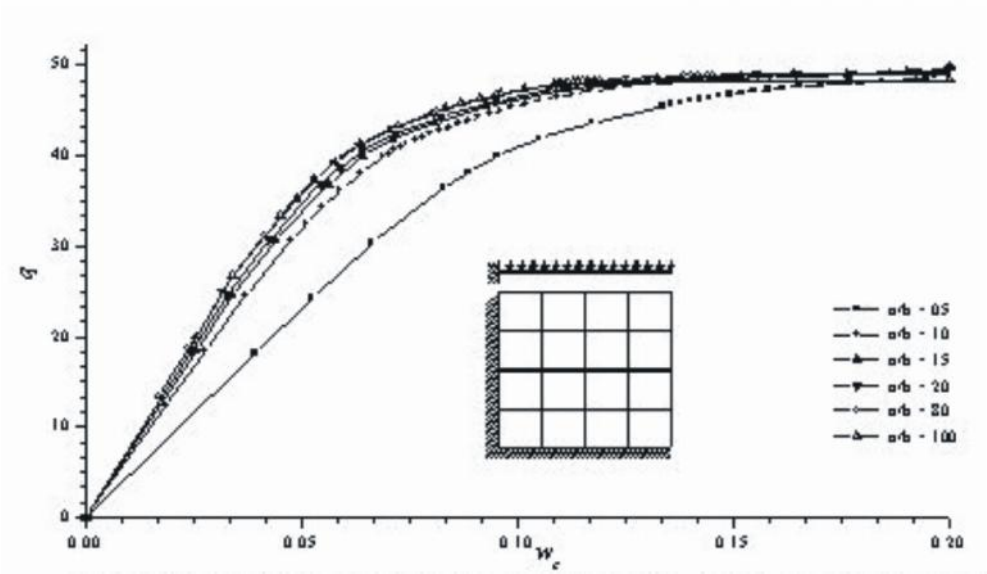

Fig. 5: Normalised load *versus* normalised central displacement for clamped circular plate with uniformly distributed load: Comparisons of different a/h ratios (HOST)

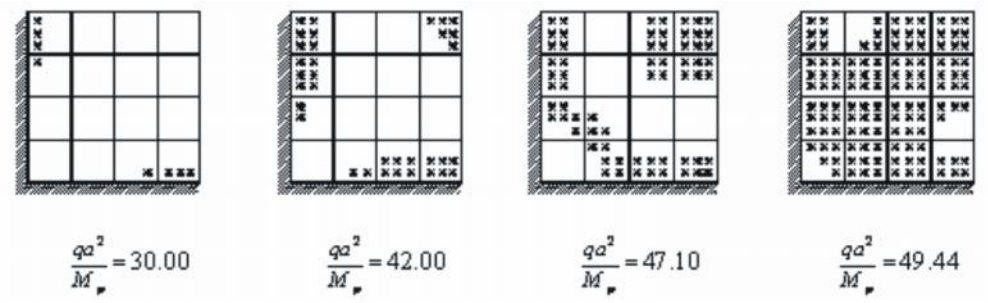

Fig. 6: Progress of plastic zone with load increments for a/h=30: Clamped circular plate with uniformly distributed load (HOST)

Table 6: Collapse loads for clamped circular plate with uniformly distributed load (E = 10.92, ν = 0.3, $\bar{q}_0$ = 1000.00 and R = 5.00)

d/h	h	Initial UDL	M_0	FOST	HOST
05	2.000	140.0	1000.0	12.74	13.18
10	1.000	30.00	250.00	12.74	13.17
15	0.667	14.00	111.22	12.75	13.12
20	0.500	10.00	62.500	12.68	13.16
50	0.200	2.250	10.000	12.70	13.17
80	0.125	1.000	3.9060	12.76	13.18
100	0.100	1.000	2.5000	12.70	13.18

Other Finite Element Analysis: 12.02 (Watanabe and Kondo [22]); 12.84 (Papadopoulos and Taylor [24]) d/h = 100
Limit Analysis: 12.50 (Hopkins and Wang [13]) 12.72 (Guowel *et al*. [16])

Table 7: Collapse loads for clamped square plate with uniformly distributed load (E = 30000.00, ν = 0.3, $\bar{q}_0$ = 30.00 and a =6.00)

d/h	h	Initial UDL	M_0	FOST	HOST
05	1.200	18.20	10.800	48.81	49.63
10	0.600	4.600	2.7000	46.66	49.68
15	0.400	2.050	1.2000	49.54	49.72
20	0.300	1.153	0.6750	49.53	49.63
50	0.120	0.185	0.1080	48.60	49.50
80	0.075	0.073	0.0422	48.42	49.43
100	0.060	0.050	0.0270	48.05	49.47

Other Finite Element Analysis: 43.34 (Watanabe and Kondo [22]), 46.486 (Papadopoulos and Taylor [24]) a/h = 100
Limit Analysis: 42.864 49.248 Upper bound (Hodge and Belytschko [15]), Lower bound (Johnson [40])

and Figueiras [20] for a/h = 30. In the elastic range the values are almost same but after inception of yielding there are deviations and HOST predicts higher collapse load.

The effect of thickness on normalised load-displacement behaviour is shown in Fig. 5. All load-displacement curves are ductile in nature. It is observed that, the difference between thin to moderately thick plates (a/h = 10, 15, 20, 50, 80 and 100) is very less in comparison to the difference between thick (a/h = 5) and thin (a/h = 100) plates. This difference gradually reduces in plastic region and the curves for all thicknesses appear to be converging to almost the same collapse load.

Spread of plastic zones during the incremental loading process for plate a/h =30 using HOST is presented in Fig. 6. Initially, plastic zones start from mid support and spread towards the corners. Next plastic zone starts from the centre of plate and spreads towards the corners of the plate. Even after meeting of these two zones, plates still exhibit resistance to loads because of partial yielding of corner elements and mid support elements. Final collapse takes place only after yielding of all the Gauss points.

Conclusions

A refined theory, based on a higher-order displacement model incorporating the warping of the transverse cross-sections, which is significant for thick plates, has been employed for the elasto-plastic analysis of thick to thin plates.

This formulation is first of its kind for for elasto-plastic analysis of thick plates. The C^o isoparametric formulation adopted is very simple and efficient as compared to other finite element formulations. HOST has predicted higher collapse load in general

References

1. Kirchhoff G R *J fur reine und angewandte Mathmatik* (Crelle) **40** (1850) 41-48
2. Reissner E *ASME J Applied Mechanics* **12** (1945) a69-a77
3. Mindlin R D *ASME J Applied Mechanics* **18** (1951) 31-38
4. Reissner E *International J Solids and Structures* **11** (1975) 569-573
5. Lo K H, Christensen R M and Wu E M *ASME J Applied Mechanics* **44** (1977) 663-668
6. Kant T *Computer Methods in Applied Mechanics and Engineering* **31**(1982) 1-18
7. Kant T, Owen D R J and Zienkiewicz O C *Computers and Structures* **15** (1982) 177-183
8. Pandya B N and Kant T *Computer Methods in Applied Mechanics and Engineering* **66** (1988) 173-198
9. Reddy J N *International Journal of Solids and Structures* **20** (1984) 881-906
10. Sokolovsky V V *Prikl Mat Mekh* **8** (1944) 141-166
11. Pell W H and Prager W *Proceedings of 1st U S National Congress of Applied Mechanics ASME* Chicago (1951) 547-550
12. Hopkins H G and Prager W *J Mechanics and Physics of Solids*, **2** (1953) 1-18
13. Hopkins H G and Wang A J *J Mechanics and Physics of Solids* **3** (1954) 117-129
14. Hodge P G *Plastic Analysis of Structures* McGraw-Hill New York (1959)
15. Hodge P G and Belytscko T *ASME Journal of Applied Mechanics* **35** (1968) 796-802
16. Guowel M, Iwaski S, Miyamoto Y and Deto H *Inter J Mechan Sci* **40** (1998) 963-076
17. Haythornthwaite R M *Proceedings of 2ndU S National Congress of Applied Mechanics ASME* (1954) 521-526
18. Armen H, Pifko A and Levine H S *NASA Contract Report* (1971) CR-1649
19. Dinis L M S, Martins R A F and Owen D R J *Proceedings of International Conference on Numerical Methods for Non-linear Problems* University of Swansea Swansea (1980) 425-442
20. Owen D R J and Figueiras J A *International Journal for Numerical Methods in Engineering* **19** (1983) 541-566
21. Reddy J N and Chandrashekhara K In: *FEICOM Proc Inter Conf Finite Elements in Comput Mechan* Indian Institute of Technology Bombay India Edited by T Kant Pergamon Press Oxford (1985) 189-209
22. Watanabe N and Kondo K *Computers and Structures* **28** (1988) 495-503
23. Kondo K and Watanabe N A *Proc Inter Conf Finite Element Methods* Shanghai China (1982) 161-166
24. Papadopoulos P and Taylor R L *Applied Mechanics Review* **43** (1990) s40-s50
25. Prasad N S and Sridhar S *Structural Engineering and Mechanics* **6** (1998) 217-227
26. Mendelson A *Plasticity Theory and Applications* Macmillan NewYork (1968)
27. Rode V R *Finite Element Incremental Elasto-plastic Analysis of Thick Plates with a Higher-order Deformation Theory* PhD Thesis Department of Civil Engineering Indian Institute of Technology Bombay (1995)
28. Owen D R J and Hinton E *Finite Element in Plasticity* Pineridge Press Swansea (1977)
29. Owen D R J and Hinton E *An Introduction to Finite Element Computations* Pineridge Press Swansea (1979)
30. Owen D R J and Hinton E *Finite Element Software for Plates and Shells* Pineridge Press Swansea (1984)
31. Hughes T R J and Cohen M *Computers and Structures* **9** (1978) 445-450
32. Hughes T R J, Cohen M and Haroun M *Nuclear Engineering and Design* **46** (1978) 203-222
33. Zienkiewicz O C, Taylor R L and Too J M *Inter J Numerical Methods in Eng* **3** (1971) 275-290
34. Liu J, Riggs H R and Tessler A *International Journal for Numerical Methods in Engineering* **49** (2000) 1065-1086
35. Papadopoulos P and Taylor R L *International Journal for Numerical Methods in Engineering* **30** (1990) 1029-1049
36. Ibrahimbegovic A and Frey F *International Journal for Numerical Methods in Engineering* **36** (1993) 303-320
37. Wanji C and Cheung Y K *International Journal for Numerical Methods in Engineering* **40** (1997) 3919-3935
38. Srinivas S and Rao A K *ASME Journal of Applied Mechanics* **40** (1973) 298-299
39. Savithri S *Linear and non-linear analysis of thick homogeneous and laminated plates* Ph D Thesis Indian Institute of Technology Madras India (1991)
40. Johnson W *International Journal of Mechanical Sciences* **11** (1969) 911-913
41. Johnson W and Mellor P B *Engineering Plasticity* Wiley Chichester (1983).